Dyes and Pigments 90 (2011) 11–20

Contents lists available at ScienceDirect

Dyes and Pigments

journal homepage: www.elsevier.com/locate/dyepig

Synthesis and characterization of novel soluble phthalocyanines with fused conjugated unsaturated groups

Gülnur Keser Karaoğlan [a], Gülşah Gümrükçü [a], Atıf Koca [b], Ahmet Gül [c,*], Ulvi Avcıata [a]

[a] Department of Chemistry, Technical University of Yildiz, Davutpasa, Istanbul 34210, Turkey
[b] Chemical Engineering Department, Engineering Faculty, Marmara University, Göztepe, Istanbul 34722, Turkey
[c] Department of Chemistry, Technical University of Istanbul, Maslak, Istanbul 34469, Turkey

ARTICLE INFO

Article history:
Received 8 September 2010
Received in revised form
1 October 2010
Accepted 3 October 2010
Available online 28 December 2010

Keywords:
Tetraamino phthalocyanine
Organic light emitting diode
Schiff base
Extended π-conjugation
Spectroelectrochemistry

ABSTRACT

The synthesis, characterization, voltammetric and spectroelectrochemical properties of a novel tetracationic metallophthalocyanine (M = Zn) containing four Schiff's base substituents attached directly on peripheral positions have been presented in this work. The new compounds have been characterized by using elemental analysis, FTIR, ^{1}H NMR, UV–Vis and MALDI-TOF MS spectroscopic data. The electrochemical, *in-situ* spectroelectrochemical, and *in-situ* electrocolorimetric measurements on precursors and end products confirm that the complexes exhibit extra electron transfer reaction assignable to the electroactive nitro, amine and Schiff's base groups in addition to the common Pc ring-based processes. Extra conjugation of amine and cinnamaldehyde groups causes both a bathochromic shift (ca. 30 nm) in Q-band maxima and a lower redox potential (ca. −400 mV) in CV measurements.

1. Introduction

Phthalocyanines are a class of macrocyclic compounds possessing a conjugated system of 18 π-electrons. The presence of a π-electron system is essential for charge-carrier transport, so they exhibit a number of unique properties, which make them of great interest in various scientific and technological areas ranging from nanotechnology to medicine [1]. There has been growing interest in the use of phthalocyanines in a variety of new high technology fields including semiconductor devices [2], Langmuir–Blodgett films [3], electrochromic display devices [4], gas sensors [5], liquid crystals [6], nonlinear optics [7], information storage [8], organic light emitting diodes (OLED) [9], photodynamic cancer therapy [10,11] and various catalytic processes [12]. At the present time, great efforts are devoted to the introduction of phthalocyanine moieties into conjugated oligomers and polymers, e.g. by the synthesis of oligo(phenylenevinylene)-bridged phthalocyanine dimers and related compounds, with respect to their application in organic electroluminescent devices, these are expected to exhibit both the unique electrical properties of the phthalocyanine and the PPV subunits [13].

A major disadvantage of Pcs is their low solubility in organic solvents or in water and it has been overcome by introducing electron-donating substituents (alkyl, alkoxy, alkylthio chains, or bulky groups), electron-withdrawing substituents (chloro, bromo, or nitro moieties) or polar ionizable groups (sulfonyl, carboxyl, amino or quaternized ammonium groups) [14–26].

Amino Pcs have been the desired compound both in dissolution and in derivatization from the reactive amino functionalities, so there has been a considerable effort to their synthesis. Amino Pcs could not be synthesized through self-condensation of the substrate containing amino groups because of the interference of amino groups in phthalonitrile cyclotetramerization. To solve the problem, two methods were usually employed. One approach was that nitro-Pc was prepared in the first place and then it was reduced to amino-derivative; the other one was that the amino group in substrate was firstly protected by acyl or tosyl groups before the substrate was cyclotetramerized to Pc, which was then hydrolyzed to amino Pc. The former method needs relatively fewer reaction steps, so it was usually preferred [14]. However, reduction of all nitro groups simultaneously to amines by reducing agents such as sodium sulfide, stannous chloride is generally not very practical and reproducible results might not be frequently obtained [27,28].

Recently, we have reported Pcs with unsaturated cinnamaldimine moieties attached to the inner core through phenoxy-bridges [29]. This paper reports a convenient procedure for the synthesis of

* Corresponding author.
E-mail address: ahmetg@itu.edu.tr (A. Gül).

0143-7208/$ – see front matter © 2010 Elsevier Ltd. All rights reserved.
doi:10.1016/j.dyepig.2010.10.002

a new water-soluble tetra-cationic zinc phthalocyanine (**6**) which contains four conjugated Schiff's base groups on peripheral positions in the phthalocyanine framework. The main scope in the preparation of this modified phthalocyanine is to maintain continuous conjugation all through the molecule. Moreover the electrochemical properties of this compound together with the other precursors have been also studied in detail by cyclic voltammetry and spectroelectrochemistry. The voltammetric, *in-situ* spectroelectrochemical, and *in-situ* electrocolorimetric characterizations are essential to decide their possible potential usage especially in the electrochemical technological applications such as electrocatalytic and electrochromic applications. Phthalocyanines with extended redox processes maintained by the attachment of electroactive substituents are the target systems for electrochemical applications of the MPcs.

2. Experimental

2.1. Instruments and chemicals

All reagents and solvents were of reagent grade quality, obtained from commercial suppliers. The solvents were stored over molecular sieves (4 Å). 4-Nitrophthalonitrile (**1**) and complexes of **2** were synthesized as given in the literatures [30,31]. The progress of the reactions was monitored by TLC (SiO_2). IR spectra were recorded on a Perkin Elmer Spectrum One FTIR (ATR sampling accessory) spectrophotometer, electronic spectra in the UV–Vis region were recorded with an Agilent 8453 UV/Vis spectrophotometer. ^{1}H NMR spectra were recorded in *d*-tetrahydrofuran on a Varian UNITY INOVA 500 MHz spectrophotometer using TMS as internal reference. Mass spectra were performed on a Bruker microflex LT MALDI-TOF MS. Melting points were determined on an Electrothermal Gallenkamp apparatus. Elemental analyses were performed on a Thermo Flash EA 1112.

2.2. Synthesis

2.2.1. [2(3),9(10),16(17),23(24)-Tetra-nitro-phthtalocyaninatozinc (II)] (**2**)

A mixture of compound **1** (600 mg, 3.466 mmol), anhydrous Zn $(CH_3COO)_2$ (159.72 mg, 0.866 mmol) and a catalytic amount of DBU in dry DMF (1 mL) was heated at 178 °C with stirring under argon atmosphere for 24 h. After cooling to room temperature, the reaction mixture was precipitated by adding methanol. The product was separated by filtration as a dark green solid. The precipitate was washed several times with methanol and ethanol to remove the unreacted starting materials and dried *in vacuo*. This compound is soluble in THF, DMF, DMSO and dioxane. Yield: 505 mg (77%); m.p. > 200 °C. FTIR υ_{max}/cm^{-1} 3066 (CH arom.), 1524, 1333 (−NO_2), 1486, 1465, 1139, 1088, 1042, 907, 847, 757, 728; ^{1}H NMR ($CDCl_3$) δ, ppm: 7.50–9.20 (12H, m, Ar–H); UV–Vis (THF): λ_{max}/nm (10^{-5} log ε, L mol^{-1} cm^{-1}): 688 (5.03), 678(5.03), 349 (5.33); Anal. Calc. for $C_{32}H_{12}N_{12}O_8Zn$ (757.904 g mol^{-1}): C, 50.71; H, 1.60; N, 22.18; Found: C, 50.62; H, 1.71; N 21.86%; MS (MALDI-TOF): *m*/*z* (100%) 757.002 $[M]^+$.

2.2.2. [2(3),9(10),16(17),23(24)-Tetraamino-phthtalocyaninatozinc (II)] (**3**)

The compound **3** was obtained by reduction of **2**. A mixture of **2** (420 mg, 0.55 mmol), hydrazine hydrate (120 mL), and catalytic amount of 10% Pd/C was refluxed in dry dioxane (70 mL) under argon atmosphere for 72 h. The cooled reaction mixture was quickly suction filtered. The residue that had been collected on the filter was discarded, and the filtrate was evaporated to dryness gently under vacuum in rotary evaporator and washed with cold water. After being dried in vacuum, the crude green product was obtained. Compound **3** is fairly soluble in THF, DMF and DMSO. Yield: 0.1806 g (51%); m.p. > 200 °C. FTIR υ_{max}/cm^{-1} 3063 (Ar–H), 3333, 3214, 1603 (−NH_2), 1493, 1456 (Ar C=C), 1253, 1091, 1045, 938, 826, 747; ^{1}H NMR ($CDCl_3$) δ, ppm: 6.42–8.52 (12H, m, Ar–H), 4.2 (8H, s, −NH_2); UV–Vis (THF): λ_{max}/nm (10^{-5} log ε, L mol^{-1} cm^{-1}): 708 (5.02), 350 (5.21); Anal. Calc. for $C_{32}H_{20}N_{12}Zn$ (637.9721 g mol^{-1}): C, 60.24; H, 3.16; N, 26.35; Found: C, 60.38; H, 3.21; N, 26.41. MS (MALDI-TOF): *m*/*z* (100%) 637.694 $[M]^+$.

2.2.3. [2,9,16,23-Tetra-(4-[(1E)-3-iminoprop-1-en-1-yl]phenyl} dimethylamino) phthtalocyaninatozinc(II)] (**5**)

A solution of **3** (130.6 mg, 0.205 mmol) in 15 mL dry THF was added dropwise to a solution of 4-(dimethylamino)cinnamaldehyde (**4**) (143.4 mg, 0.818 mmol) in 10 mL dry THF and the mixture was refluxed under argon for 15 h. The solvent was evaporated to 1/10 of the initial volume and the reaction mixture was precipitated by adding methanol at room temperature. The product was separated by filtration as a green solid. The precipitate was washed several times with cold water methanol and ethanol to remove the unreacted starting materials and dried *in vacuo*. After being dried in vacuum, the crude dark green product was isolated with column chromatography over silica gel using $CHCl_3$: MeOH (8:1) as eluent system. Compound **5** is fairly soluble in THF, acetone, DMF and DMSO, $CHCl_3$. Yield: 60 mg (23%); m.p. > 200 °C. FTIR υ_{max}/cm^{-1} 3058 (Ar–H, w), 2954–2871 (−CH_3, s), 1605 (−N=CH, m), 1564, 1482 (Ar C=C), 1430, 1153, 859. ^{1}H NMR ($CDCl_3$) δ, ppm: 6.64–8.45 (m, 28H, Ar–H), 3.14 (s, 24H, −NCH_3), 6.56–8.01 (m, 12H, =CH–); UV–Vis (THF): λ_{max}/nm (10^{-5} log ε, L mol^{-1} cm^{-1}): 705 (5.041), 422 (5.48), 357 (5.25); Anal. Calc. for $C_{76}H_{64}N_{16}Zn$ (1266.8376 g mol^{-1}): C, 72.05; H, 5.09; N, 17.69; Found: C, 72.11; H, 5.02; N, 17.70. MS (MALDI-TOF): *m*/*z* (100%) 1265.838 $[M-H]^+$, 1178 $[M-2[N(CH_3)_2]]^+$, 1093.6 $[M-[N(CH_3)_2{-}Ar{-}C{=}C{-}C{=}N{-}]]^+$, 1090.53 $[M-4[N(CH_3)_2]]^+$.

2.2.4. Tetrakis-(4-[(1E)-3-iminoprop-1-en-1-yl]-N,N, N-trimethylphenylammonium) phthalocyaninato zinc(II)] tetraiodide (**6**)

Compound **5** (40 mg, 0.032 mmol) was dissolved in $CHCl_3$ (6.5–7.0 mL) and CH_3I (15.66 mg, 0.11 mmol) was added to this solution. The mixture was refluxed for 6 h. Then the mixture was filtered and the precipitate was washed with $CHCl_3$. The precipitate was dried *in vacuo*. Compound **6** is fairly soluble in THF, acetone, DMF, DMSO, $CHCl_3$, methanol and water. Yield: 27.8 mg (48%); m.p. > 200 °C. FTIR υ_{max}/cm^{-1} 3032 (Ar–H, w), 2945–2851 (−CH_3, m), 1603 (−HC=N, s), 1568, 1478 (Ar C=C); ^{1}H NMR ($CDCl_3$) δ, ppm: 7.20–8.50 (m, 28H, Ar–H), 4.09 (s, 36H, −NCH_3), 6.68–8.05 (m, 12H, =CH–); UV–Vis (THF): λ_{max}/nm (10^{-5} log ε, L mol^{-1} cm^{-1}): 711 (4.98), 422 (5.40), 355 (5.07); Anal. Calc. for $C_{80}H_{76}N_{16}ZnI_4$ (1326.97 + 508 = 1834.973 g mol^{-1}): C, 72.55; H, 5.86; N, 16.71; Found: C, 72.92; H, 5.26; N, 16.43; MS (MALDI-TOF): *m*/*z* (%) 1280.804 $[M-(N{-}(CH_3)_3{-}Ar{-}C{=}C{-}C{=})-3I^-]$, 1137.507 $[M-(N(CH_3)_3{-}Ar{-}C{=}C{-}C{=}N)-4I^- - H]^+$, 1326.971 $[M-4I^-]^{4+}$.

2.3. Electrochemical measurements

The cyclic voltammetry (CV) and square wave voltammetry (SWV) measurements were carried out with Gamry Reference 600 potentiostat/galvanostat controlled by an external PC and utilizing a three-electrode configuration at 25 °C. The working electrode was a Pt disc with a surface area of 0.071 cm^2. A Pt wire served as the counter electrode. Saturated calomel electrode (SCE) was employed as the reference electrode and separated from the bulk of the solution by a double bridge. Electrochemical grade TBAP in extra

pure DMSO was employed as the supporting electrolyte at a concentration of 0.10 mol dm^{-3}.

2.4. In-situ spectroelectrochemical and in-situ electrocolorimetric measurements

UV–Vis absorption spectra and chromaticity diagrams were measured by an OceanOptics QE65000 diode array spectrophotometer. *In-situ* spectroelectrochemical measurements were carried out by utilizing a three-electrode configuration of thin-layer quartz thin-layer spectroelectrochemical cell at 25 °C. The working electrode was a Pt tulle. Pt wire counter electrode separated by a glass bridge and a SCE reference electrode separated from the bulk of the solution by a double bridge were used. *In-situ* electrocolorimetric measurements, under potentiostatic control, were obtained using an OceanOptics QE65000 diode array spectrophotometer at color measurement mode by utilizing a three-electrode configuration of thin-layer quartz spectroelectrochemical cell. The standard illuminant A with 2 degree observer at constant temperature in a light booth designed to exclude external light was used. Prior to each set of measurements, background color coordinates (*x*, *y*, and *z* values) were taken at open-circuit, using the electrolyte solution without the complexes under study. During the measurements, readings were taken as a function of time under kinetic control, however only the color coordinates at the beginning and final of each redox processes were reported.

3. Results and discussions

3.1. Synthesis and characterization

The phthalocyanine with a Schiff base group (**5**) was prepared by a three step procedure. The critical precursor in this reaction sequence is the tetraamino-Pcs derivative which has been successfully prepared by the reduction of tetra-nitro-Pc with hydrazine hydrate in the presence of palladium/active carbon (10%) as the catalyst. In our hands, this method has been proven to be more reproducible with moderate yields than the reported reduction processes with sodium sulfide or stannous chloride [27,28].

4-Nitrophthalonitrile (**1**) which has been synthesized as given the literature [30] is a suitable starting material for various substituted phthalocyanines. The cyclotetramerization of (**1**) with zinc (II) acetate in the presence of DBU as a strong base results in the formation of compound (**2**) [31]. The second step was the reduction of nitro groups on the periphery (**2**) to amines in the presence of hydrazine hydrate and 10% Pd/C in a period of 72 h under reflux. The green compound (**3**) was purified by washing successively with water, cold methanol and ethanol and then drying *in vacuo*. The Schiff base phthalocyanine (**5**) was obtained by the reaction of compound (**3**) and 4-(dimethylamino)cinnamaldehyde (**4**) in the presence of THF in 23% yield (Fig. 1).

Conversion of tertiary amine functionality to quaternary ammonium group on the periphery led to phthalocyanine derivative soluble in water. When the Schiff base phthalocyanine (**5**) was treated with methyl iodide in chloroform, the hygroscopic Schiff's base phthalocyanine product with tetra quaternary ammonium group (**6**) was obtained in 48% yield (Fig. 2).

Characterization of the products involved a combination of methods by elemental analysis, ^{1}H NMR, UV–Vis, MALDI-TOF MS and IR spectroscopy.

Spectral investigations on the newly synthesized compounds are in accordance with the proposed structures (Figs. 1 and 2). Cyclotetramerization of dinitriles was confirmed by the disappearance of the sharp (–C≡N) vibrations at 2238 cm^{-1} of (**1**). IR

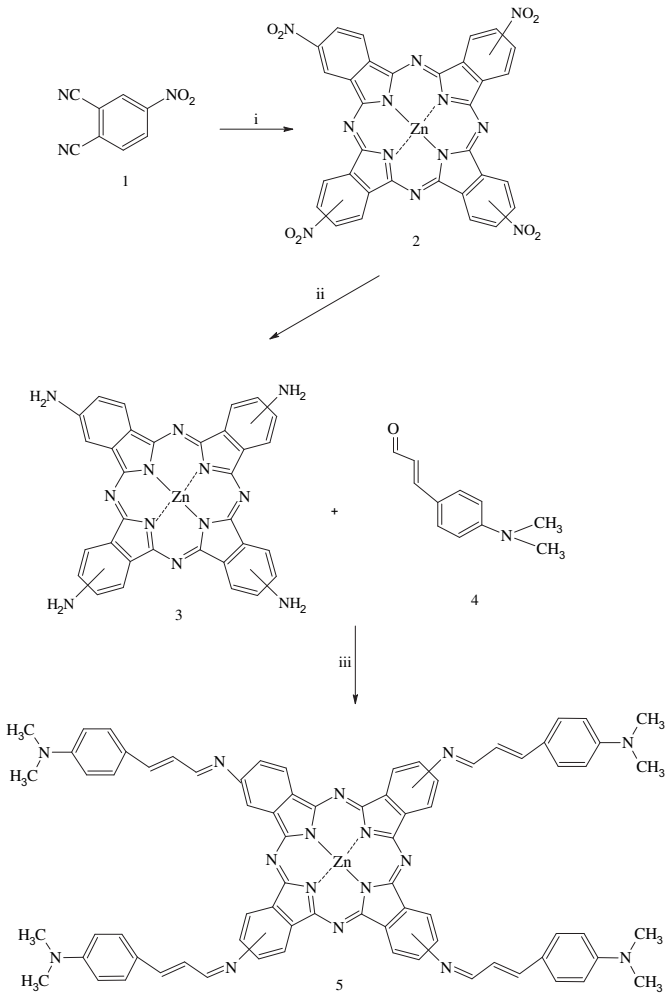

Fig. 1. Synthesis of Pcs. (i) DBU, DMF, $Zn(OAc)_2$; (ii) Pd/C, hydrazine hydrate, dioxane; (iii) THF, reflux.

spectrum of to 2 indicated the presence of $-NO_2$ groups by the intense stretching bands at 1524, 1333 cm^{-1}.

The $-NH_2$ group in **3** was observed with stretching vibrations at 3333 and 3214 cm^{-1} as an intense doublet and bending vibrations at 1603 cm^{-1} as a strong peak.

The IR spectrum of the **5** showed characteristic Schiff's base stretching band at 1605 cm^{-1}. This intense band is assigned to the –C=N stretching frequency of ligand and is characterized for the azomethine moiety of most Schiff's base compounds. The absorption band of the C=O in the 4-(dimethyl amino)-cinnamaldehyde disappeared in the infrared spectrum of the **5**, which indicates that the

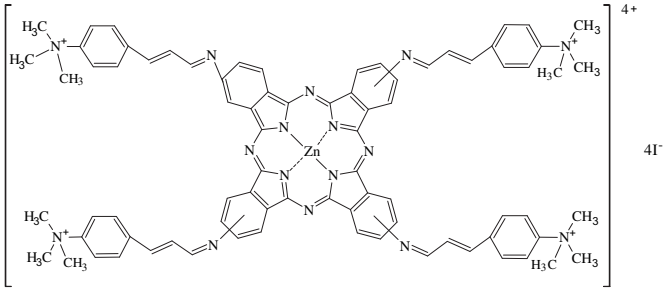

Fig. 2. Quaternized zinc phthalocyanine (**6**).

condensation has occurred. IR spectrum of tetra-cationic phthalocyanine (**6**) showed $-CH_3$ bands at 2945–2851 cm^{-1}.

The ^1H NMR spectrum of (**2**) indicates aromatic protons as two multiplets around 7.50–9.20 ppm. Compound **3** exhibited aromatic protons at δ 6.42–8.52 ppm as a multiplet and the $-NH_2$ protons at δ 4.2 ppm. The aromatic protons for **5** and **6** appeared between at 6.64–8.45 and 7.20–8.50 ppm as a multiplet, respectively. $-NCH_3$ protons appear as a singlet at δ 3.14 in **5**. The protons of =CH groups were observed in the range δ 6.56–8.01 ppm for **5** and δ 6.68–8.05 ppm for **6**.

The best indications for phthalocyanine systems are given by their UV–Vis spectra in solution (Fig. 3). The UV–Vis spectra of the phthalocyanines in THF showed the typical pattern, mainly π–π^* transition of the tetrapyrrole units forming in the central core of the phthalocyanine: intense Q-absorption band in the visible region of around 678–711 nm and Soret or B band in the ultraviolet region of around 349–357 nm. The characteristic Q-band absorption of metallophthalocyanines with D_{4h} symmetry is observed as a single band of high intensity in the visible region [32]. A big shift between the Q-band absorption peaks of the two species **2** and **3** is a consequence of change in electron density between electron-withdrawing $-NO_2$ group into $-NH_2$ on peripheral positions. Spectra of **3** and **5** in THF are very similar, with intense Q bands at 708 and 705 nm due to a single $\pi \rightarrow \pi^*$ transition with shoulders at 636 and 636 nm, respectively. However, the Soret (B) bands are observed at different wavelengths as 350 and 357 nm, respectively.

UV–Vis spectra of the quaternized phthalocyanine compound **6** in THF is similar to those of corresponding non-quaternized derivative **5** in THF. First, the B band is slightly shifted to shorter wavelength. Second, the Q band is slightly shifted to longer wavelength. However, the electronic spectra of the quaternized phthalocyanine **6** in water showed some differences from those in THF as a result of solvent effect.

Spectral changes occurring as a result of enhanced conjugation have been clearly shown when the electronic spectra of Pcs (**2**–**6**) are compared with those of analogous molecules where identical substituents are attached not directly the Pc core but through phenylene-oxy bridges. As expected, Q bands of Pcs with conjugated cinnamaldimine groups show bathochromic shifts of about 27–32 nm (Table 1).

Quaternized zinc Pc **6** showed enhanced solubility in a wide range of solvents, so it has become possible to investigate their

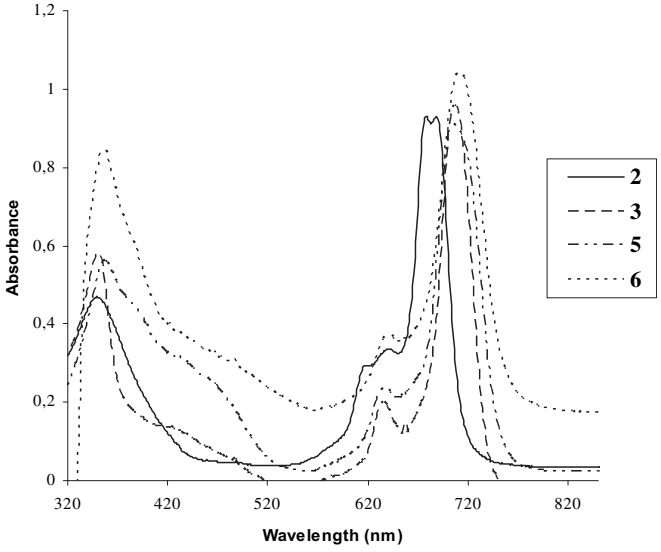

Fig. 3. UV–Vis spectra of phthalocyanines in a THF solution for **2**, **3**, **5** and **6**.

Table 1
Location of the Q bands (in nm) of Pc derivatives **2**, **3**, **5**, **6** and (**4′**, **5′**, **7′**, **8′**) those with identical substituents attached through phenyleneoxy-bridges (nitro, amino, cinnamaldimine, quaternized cinnamaldimine) in Ref. [29] in THF.

Compound/substituents	λ, nm (log ε, L mol^{-1} cm^{-1})		
2 Nitro	616[a] (4.46)	678 (4.97)	683 (4.55)
3 Amino	636[a] (4.30)	708 (4.98)	
5 Cinnamaldimine	636[a] (4.37)	705 (4.96)	
6 Quaternized cinnamaldimine	642[a] (4.57)	711 (5.02)	
4′ Nitro	607[a] (4.30)	672 (4.96)	
5′ Amino	613[a] (4.34)	679 (5.06)	
7′ Cinnamaldimine	612[a] (4.23)	678 (4.97)	
8′ Quaternized cinnamaldimine	613[a] (4.50)	679 (5.02)	

[a] Shoulder.

electronic properties with respect to solvent polarity and donor properties (Table 2). Among the solvents studied highest shift in Q-band absorption was observed in the case of donor solvents such as pyridine and DMSO. Methanol < THF < DMF order can be given for the other relatively polar solvents.

3.2. Electrochemical measurements

It is obviously documented that the phthalocyanine ring often can be reduced up to tetraanionic and oxidized up to dicationic states. In addition to the Pc ring-based redox reactions, redox-active metal ions, such as Co^{II}, Fe^{II} and Mn^{II}, in the core of the Pc and redox-active substituents such as pyridine, ferrocene and nitro, typically show additional redox couples. Here we carried out electrochemical characterization of the sequentially synthesized ZnPc complexes bearing redox-active substituents, nitro (**2**), amino (**3**), 4-(dimethylamino)cinnamaldimine (**5**) and its quaternized form (**6**). CV responses of the complexes were used to support the proposed structures of the newly synthesized phthalocyanine complexes (**2**–**6**) by comparing with each other and with the similar MPc in the literature [33–36]. Table 3 lists the assignments of the redox couples and estimated electrochemical parameters including the half-wave peak potentials ($E_{1/2}$), ratio of anodic to cathodic peak currents (I_{pa}/I_{pc}), peak to peak potential separations (ΔE_p), and difference between the first oxidation and reduction processes ($\Delta E_{1/2}$).

Fig. 4 illustrates CVs and SWVs of **2** in DMSO/TBAP electrolyte on a Pt working electrode. Complex **2** exhibits two sequential one-electron Pc ring reductions, $[Zn^{II}Pc^{-2}]/[Zn^{II}Pc^{-3}]^-$ ($R._{(Pc1)}$ at $E_{1/2} = -0.81$ V) and $[Zn^{II}Pc^{-3}]^-/[Zn^{II}Pc^{-4}]^{2-}$ ($R._{(Pc2)}$ at $E_{1/2} = -1.40$ V), and a one-electron ring oxidation, $[Zn^{II}Pc^{-2}]/[Zn^{II}Pc^{-}]^+$ ($Oxd._{(Pc1)}$ at $E_{1/2} = 1.02$ V). In addition a one-electron reduction of four nitro groups (ZnPc–4[R–NO_2]/ZnPc–4[R–NO_2]$^{*-}$ ($Red._{NO_2}$ at $E_{1/2} = -1.20$ V)) is recorded between two ring reduction processes. It is well documented that nitro groups give a 1-electron reduction processes at around −1.0 V vs. SCE in aprotic media depending on the substituents and electrolyte system [37–39]. Observation of a wave before the firs reduction process ($R._{(Pc1)}$) may be due to the aggregation of the complex. As shown in Fig. 4b, current intensity of this wave decreases more than the other

Table 2
Location of the Q bands (in nm) of quaternized Pc derivative **6** in different solvents.

Compound	λ, nm (log ε, L mol^{-1} cm^{-1})	
Methanol	640[a] (4.50)	708 (4.79)
THF	642[a] (4.57)	711 (5.02)
Pyridine	649 [a] (4.68)	720 (5.22)
DMF	640[a] (4.48)	714 (5.06)
DMSO	647[a] (4.52)	720 (4.98)

[a] Shoulder.

Table 3
Voltammetric data of the complexes.

Complex		$O_{\cdot(s1.)}$[f]	$O_{\cdot(Pc2)}$	$O_{\cdot(Pc1)}$	$R_{\cdot(Pc1)}$	$R_{\cdot(Pcs2)}$	$R_{\cdot(s1)}$[g]	$R_{\cdot(s2)}$[h]	$\Delta E_{1/2}$[d]
2	$E_{1/2}$[a] vs. SCE	–		1.02[e]	−0.81 (−0.62)	−1.40	−1.11		1.64
	ΔE_p[b] (mV)			–	61	180	110		
	I_{pa}/I_{pc}[c]			–	0.85	0.50	0.90		
3	$E_{1/2}$[a] vs. SCE	1.05[e]	0.57	0.19	−1.26	−1.63			1.45
	ΔE_p[b] (mV) vs. SCE	–	100	60	60	120			
	I_{pa}/I_{pc}[c]	–	0.45	0.90	0.99	0.55			
5	$E_{1/2}$[a] vs. SCE	0.82	0.62	0.20	−1.23 (−1.11)	−1.71			1.31
	ΔE_p[b] (mV)	170	–	70	63	90			
	I_{pa}/I_{pc}[c]	0.71	–	0.93	1.10	0.92			
6	$E_{1/2}$[a] vs. SCE	0.30	0.96	0.54	−1.24 (−1.05)	−1.84			1.35
	ΔE_p[b] (mV)	46	140	130	67	140			
	I_{pa}/I_{pc}[c]	0.71	0.75	0.77	0.92	0.62			

[a] $E_{1/2} = (E_{pa} + E_{pc})/2$ at 0.100 V s^{-1}.
[b] $\Delta E_p = E_{pa} - E_{pc}$ at 0.100 V s^{-1}.
[c] I_{pa}/I_{pc} for reduction, I_{pc}/I_{pa} for oxidation processes at 0.100 V s^{-1} scan rate.
[d] $\Delta E_{1/2} = \Delta E_{1/2}$ (first oxidation) − $\Delta E_{1/2}$ (first reduction) = HOMO–LUMO gap for metallophthalocyanines having electro-inactive metal center.
[e] The process is irreversible, thus E_p values were given as $E_{1/2}$.
[f] $Oxd._{(Subs.)}$ process is the oxidation of the amine groups of the complex **5** and iodide oxidation for the complex **6**.
[g] $Red._{(subs)1}$ processes are the reduction of the cinnamaldehyde groups for the complexes **5** and **6**.
[h] $Red._{(subs)2}$ processes are the reduction of the nitro groups for the complex **2** and triiodide reduction for the complex **6**.

peaks with dilution which support the aggregation behavior of the complex. UV–Vis spectra of the complex illustrated the aggregation behavior of the complex, which is discussed in spectroelectrochemical measurement section. ΔE_p and I_{pa}/I_{pc} values of the reduction processes indicate that while the first and second peaks have reversible character, third reduction process ($R_{\cdot(Pc2)}$) is irreversible even at very slow scan rates. While I_{pa}/I_{pc} values of the first reduction process are close to unity at slow scan rates, they decreases with increasing scan rates, which indicates existence of a chemical reaction succeeding the electron transfer reaction. This chemical reaction may be the aggregation-disaggregation equilibrium of the complex. Assignments of the redox processes were confirmed with in-situ spectroelectrochemical measurements given below and with comparing with the similar MPcs in the literature [33–36].

Replacement of the nitro groups of the ZnPc (**2**) with amino groups (complex **3**) changes the electrochemical responses of the complex considerably. Fig. 5 illustrates the CV and SWV response of the complex **3**. When compared with the voltammetric responses of the complex **4**, the redox couple assigned to the nitro reduction is disappeared, aggregation of the complex is not recorded and all redox processes shift to negative potentials due to the replacement of the electron-withdrawing nitro groups with the electron releasing amino groups. As shown in Fig. 5, the complex **3** gives two common 1-electron reversible Pc ring-based reduction processes,

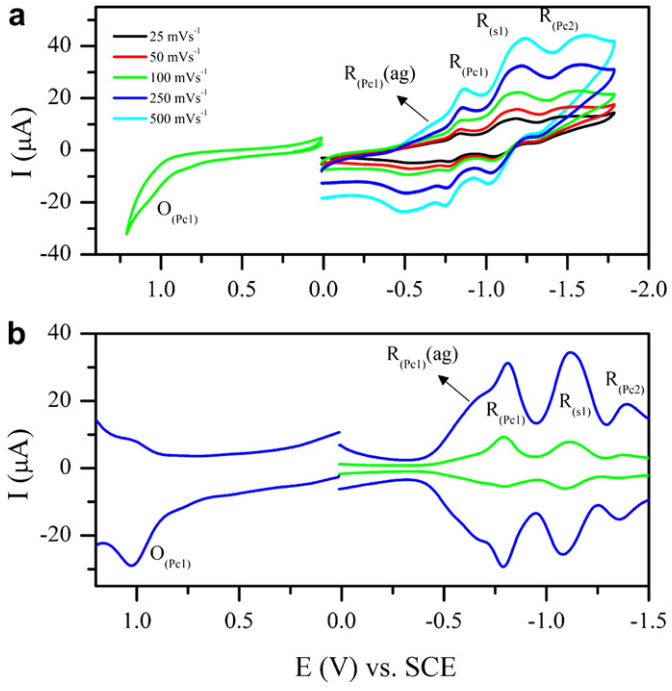

Fig. 4. **a**) CVs of **2** (5.0×10^{-4} mol dm^{-3}) at various scan rates on a Pt working electrode in DMSO/TBAP. **b**) SWV of **2** recorded different concentrations (blue = 5.0×10^{-4} mol dm^{-3}; red = 1.0×10^{-4} mol dm^{-3}). SWV parameters: step size = 5 mV; pulse size = 100 mV; frequency = 25 Hz.

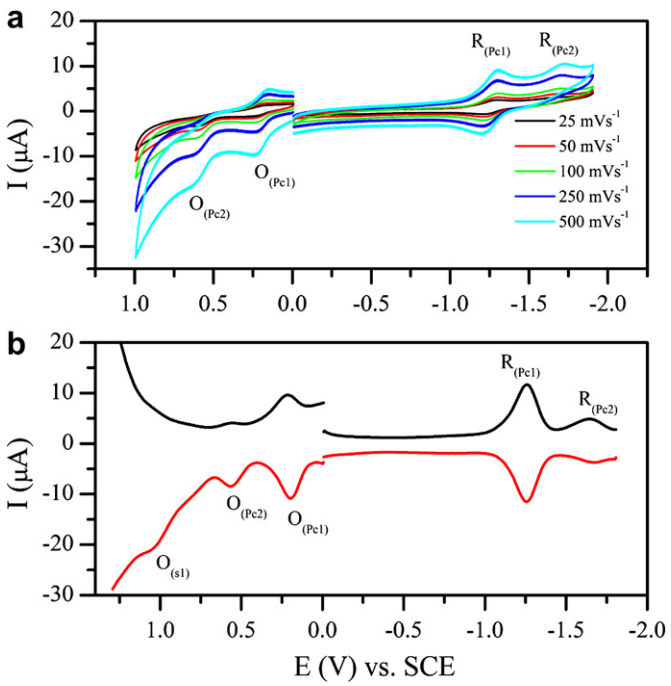

Fig. 5. **a**) CVs of **3** (5.0×10^{-4} mol dm^{-3}) at various scan rates on a Pt working electrode in DMSO/TBAP. **b**) SWV of **3**.

$R_{\cdot(Pc1)}$ ($E_{1/2} = -1.26$ V) and $R_{\cdot(Pc2)}$ ($E_{1/2} = -1.63$ V) during the cathodic scans. In the anodic scans, while two common Pc ring-based oxidation processes are recorded at 0.19 V and 0.57 V with the CV measurements, a third oxidation process is recorded with SWV at 1.05 V which could be assigned to the oxidation of the amine groups on the complex **5**. It is documented that amine substituents give oxidation process at around 1.0 V in aprotic media [36,39,40].

The complex **5** is the products of the reaction between the complex **3** and 4-(dimethylamino)cinnamaldehyde (Fig. 1). Changing of the amino groups (complex **3**) with 4-(dimethylamino) cinnamaldehyde (complex **5**) was also monitored electrochemically. Fig. 6 shows the CV and SWV responses of the complex **5**. When we compared CV responses of the complex **5** with its starting complex **3**, it is shown that while amine oxidation process of the complex **3** at 1.05 V disappears, a new quasi-reversible 4-electron oxidation couples (1-electron for each cinnamaldehyde group) at 0.82 V is observed in addition to the common Pc-based electron transfer processes, reversible first reduction at −1.23 V ($R_{\cdot(Pc1)}$), quasi-reversible second reduction at −1.71 V ($R_{\cdot(Pc2)}$), reversible first oxidation at 0.20 V ($O_{\cdot(Pc1)}$) and irreversible second ring oxidation at 0.62 V ($O_{\cdot(Pc2)}$). Assignments of the redox processes were confirmed with in-situ spectroelectrochemical measurements given below. As shown in Fig. 7, the complex **5** is electropolymerized on the working electrode during the continuous CV cycles. Observation of new enhancing waves and increasing of the prevalent peaks with shifting during the continuous CV cycles are indicators of a polymerization mechanism [41,42]. It was shown that switching potential of the CV measurements affected the polymerization mechanism of the complex. A polymerization process was not recorded, when the switching potential was before the third oxidation potential. However electropolymerization process was observed, when the positive switching potential passed the third oxidation process. These findings indicated that oxidation of the cinnamaldehyde groups initiate the polymerization process.

Fig. 8 shows the CV response of the complex **6**. Quaternization of the complex **5** to form the complex **6** does not affect the electron

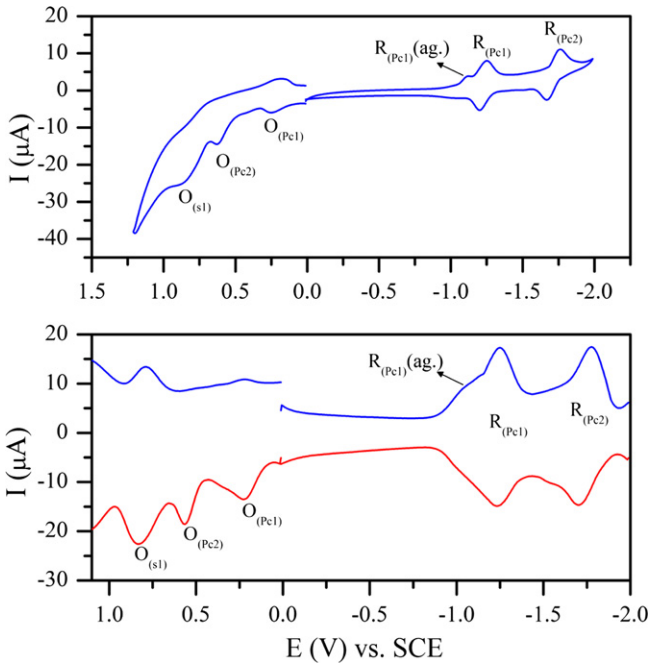

Fig. 6. **a**) CVs of **5** (5.0×10^{-4} mol dm^{-3}) at 0.100 V s^{-1} scan rate on a Pt working electrode in DMSO/TBAP. **b**) SWV of **5**.

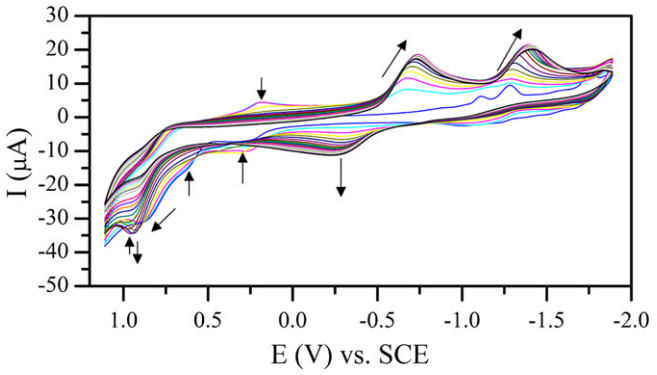

Fig. 7. CVs recorded with repetitive cycles of **5** at 0.100 V s^{-1} scan rate on a Pt working electrode in DMSO/TBAP.

transfer processes of the Pc-based redox processes considerably. But presence of iodide ions in the complex confuses the CV and SWVs due to the electron transfer processes of the species I^-, I_2 and I_3^- which are present in equilibrium. It is well documented that iodide ions give two redox processes [43–45], which are easily monitored at 0.30 V ($2I^-/I_2$) and −0.73 V ($I^-_3/3I^-$). During the first CV scan from −0.50 V to −2.00 V, the complex **6** gives two Pc ring-based reduction processes at −1.24 V ($R_{\cdot(Pc1)}$) and −1.84 V ($Red._{\cdot(Pc2)}$). However when repetitive CV scans in all available potential window of the electrolyte system is performed, in addition to the reduction processes the complex **6** gives iodide-based electron transfer processes at 0.30 V and −0.73 V and Pc ring-based oxidation processes at 0.60 V ($R_{\cdot(Pc1)}$) and 0.96 V ($R_{\cdot(Pc1)}$). During the repetitive CV scans, peak currents of the redox processes increases with continuous CV cycles, which indicate electrodeposition of the complex on the working electrode. SWV of the complex given in Fig. 7b indicates the electrochemical responses of the complex and effects of the switching potential to the electrochemical responses

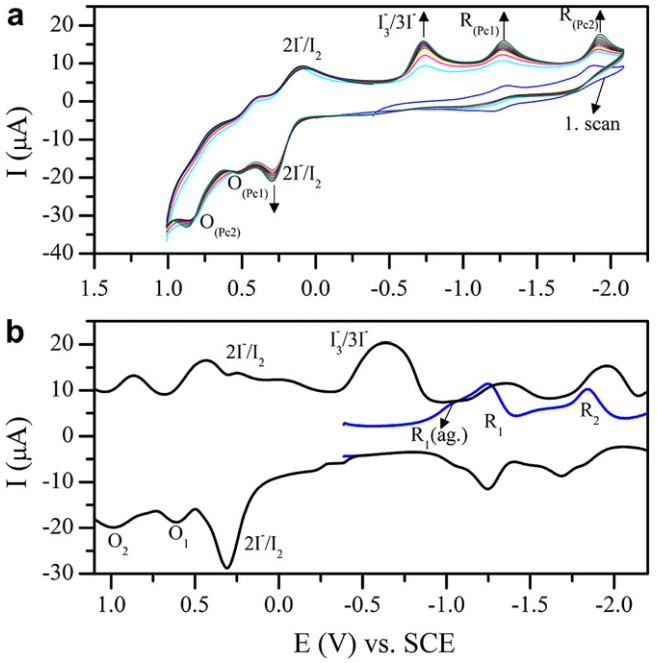

Fig. 8. **a**) CVs recorded with repetitive cycles of **6** at 0.100 V s^{-1} scan rate on a Pt working electrode in DMSO/TBAP. **b**) SWV of **6**. Black SWV between 1.20 V and −2.20 V; Blue SWV between 1.20 V and −2.20 V.

of the complex. Similar CV responses for the effects of iodide were recorded in our previous papers [46]. Addition of iodide ions enhances the peak currents of the relevant peaks, which supported our assignments. When compared with the complex **5**, the Pc ring-based oxidation processes of the complex **6** shift to positive potentials due to the oxidation of the iodide before these processes. Assignments of the redox processes were confirmed with in-situ spectroelectrochemical measurements given below.

3.3. Spectroelectrochemical studies

Spectroelectrochemical studies were employed to confirm the assignments in the CVs of the complexes. The complexes **2**, **3**, **5**, and **6** have all redox inactive metal centers. Therefore, in-situ UV–Vis spectral changes of them indicate the Pc ring-based and/or substituent-based redox characters. The complexes **2** and **3** give very similar spectral changes due to the similarity of the redox processes. The only difference between spectral changes between **2** and **3** is the aggregation property of the complex **2**. Any spectral changes were recorded under the applied potential at −1.25 V (reduction of nitro groups) for the complex **2**, which indicates that reduction of the nitro groups do not affect the spectrum of the complex **2**. Fig. 9 shows the in-situ UV–Vis spectral changes of **3** under the controlled potential application. During the potential application at −1.40 V, two distinct spectral changes are observed. At the beginning of the reduction process, while the Q band at 725 nm decreases without shifting a new band in the ligand to metal charge transfer (LMCT) region at 551 nm is recorded. Then at the same potential application, new bands are observed at 400, 600 and 653 nm while the Q band at 725 nm decreases without shifting. These characteristics spectral changes are indicator of the ring-based redox processes and assigned to $[Zn^{II}Pc^{-2}]/[Zn^{II}Pc^{-3}]^{-1}$ (Fig. 9a) [47–50]. Two different spectral changes may due to the constitutional changes of the reduced species with a succeeding chemical reaction. Due to the possible constitutional changes, the process does not give clear isosbestic points. While well resolved isosbestic points are recorded at 377, 484, 652, and 804 nm at the beginning of the process, these isosbestic points shift to 367, 443, 533, 677, and 782 nm. Smaller peak current of the second reduction process with respect to the first on in the CV and SWV of the complex in Fig. 5 may due to this chemical reaction succeeding the first electron transfer reaction.

Then at the −1.80 V potential applications, two different spectral changes are also recorded like the spectral changes at −1.35 V. These different spectral changes may be due to the presence of two different reduced species formed during the first reduction reaction. As shown in Fig. 9b, first of all, while the band at 600 nm increases in intensity, the band at 653 nm starts to decreases. At the same time two new bands appear at 550 and 905 nm, while the Q band and the B band at 400 nm decrease in intensity. Then the

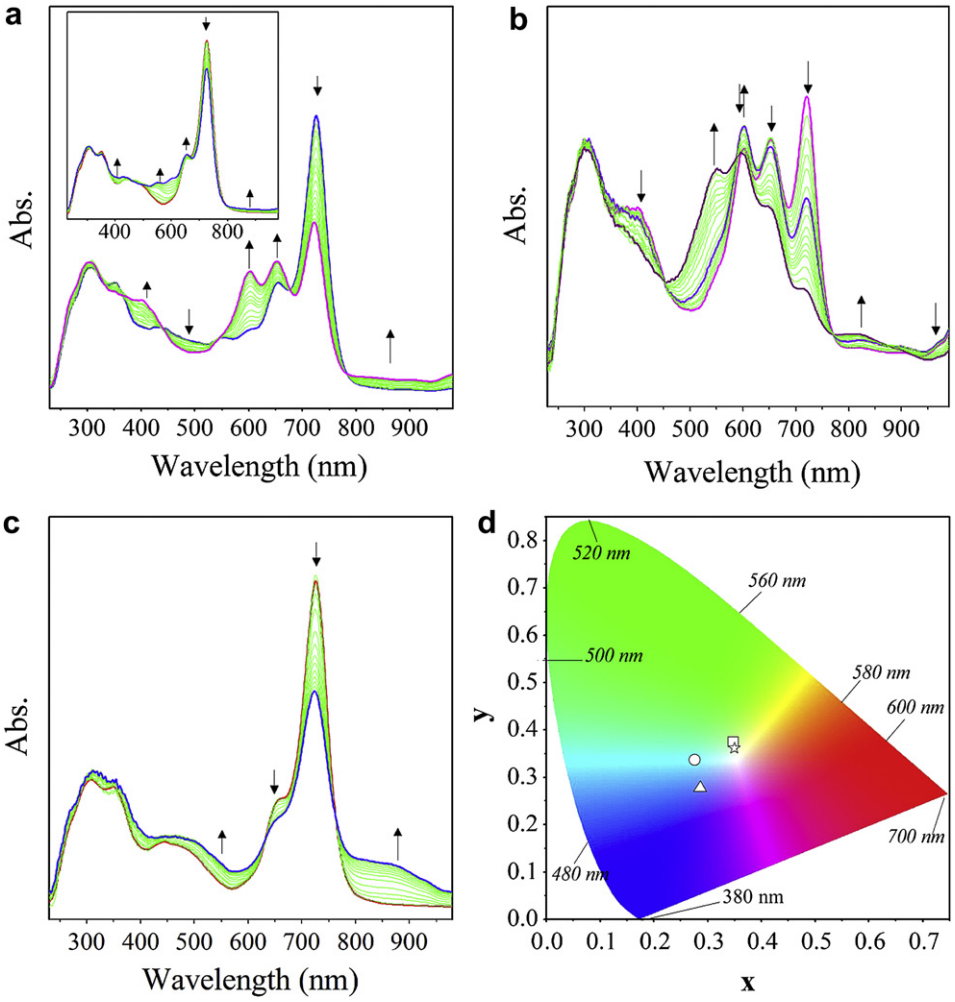

Fig. 9. *In-situ* UV–Vis spectral changes of **3**. **a**) $E_{app} = -1.40$ V (inset: initial part of the spectra). **b**) $E_{app} = -1.80$ V. **c**) $E_{app} = 0.30$ V. **d**) Chromaticity diagram (each symbol represents the color of electro-generated species; □: $Zn^{II}Pc^{-2}$, ○: $Zn^{II}Pc^{-3}$, △: $Zn^{II}Pc^{-4}$, ☆: $Zn^{II}Pc^{-1}$.

bands at 600 and 905 nm start to decreases while the remaining part of the spectrum continues to initial trend. When the whole spectral changes are compared with the similar complexes in the literature, these spectroscopic changes are easily assigned to the reduction of the monomeric species in different forms, $[Zn^{II}Pc^{-3}]^{-1}$ to $[Zn^{II}Pc^{-4}]^{-2}$ dianionic species (Fig. 9b) [47–51]. Spectroscopic changes given in Fig. 9c are characteristics of the oxidation of $[Zn^{II}Pc^{-2}]$ to monocationic $[Zn^{II}Pc^{-1}]^{+1}$ species [47–51]. During the potential application at 0.70 V, all bands decreased in intensity which indicates decomposition of the complex under 0.70 V applied potential.

The color change of the complexes during the redox processes were recorded using in-situ colorimetric measurements. Fig. 9d gives the chromaticity diagrams of the complex **3** recorded simultaneously during the spectroelectrochemical measurements. Without any potential application, the solution of **3** is light green ($x = 0.349$ and $y = 0.374$). As the potential is stepped from 0 to −1.40 V color of neutral **3**, $[Zn^{II}Pc^{-2}]$ start to changes and greenish blue color ($x = 0.276$ and $y = 0.337$) of monoanionic form of **3** was obtained at the end of the first reduction. Similarly color of the dianionic species was recorded as blue ($x = 0.286$ and $y = 0.276$) and monocationic species, $[Zn^{II}Pc^{-1}]^{+1}$ has yellowish green color ($x = 0.350$ and $y = 0.361$). Measurement of the *xyz* coordinates allows quantification of each color of redox species that is very important to decide their possible electrochromic application.

In-situ UV–Vis spectral changes of the complex **5** are approximately same with those of the complex **3**. During the potential application at −1.40 V, while the Q band at 726 nm decreases in intensity without shifting a new band in the LMCT region at 606 nm is recorded. At the same time the band assigned to the $n-\pi^*$ transition at 652 nm increases in intensity. Moreover while the B band shifts from 374 to 401 nm with increasing, the NIR region of the spectrum after 800 nm increases in intensity. Well resolved isosbestic points are recorded at 350, 449, 515, 670, and 781 nm. Initial light green color ($x = 0.381$ and $y = 0.415$) of the solution changed to bluish green ($x = 0.313$ and $y = 0.400$) at the end of the firs reduction process. These characteristics spectral changes are indicator of the ring-based redox processes and assigned to $[Zn^{II}Pc^{-2}]/[Zn^{II}Pc^{-3}]^{-1}$ (Fig. 10a) [47–51]. Then at the −1.80 V potential application, while the bands at 606 and 652 nm decreases in intensity, a new band at 5550 nm starts to appear. At the same time, the Q and B bands decrease in intensity without shifting (Fig. 10b). Well resolved isosbestic points at 345, 470, 595, and 782 nm and color changes from bluish green ($x = 0.313$ and $y = 0.400$) to light blue color ($x = 0.322$ and $y = 0.322$) are recorded. These spectroscopic changes are easily assigned to the reduction of the monomeric species $[Zn^{II}Pc^{-3}]^{-1}$ to $[Zn^{II}Pc^{-4}]^{-2}$ dianionic species (Fig. 10b) [47–51]. Spectroscopic changes given in Fig. 9c are characteristics of the oxidation of $[Zn^{II}Pc^{-2}]$ to monocationic $[Zn^{II}Pc^{-1}]^{+1}$ species. During the potential application at 1.00 V, all

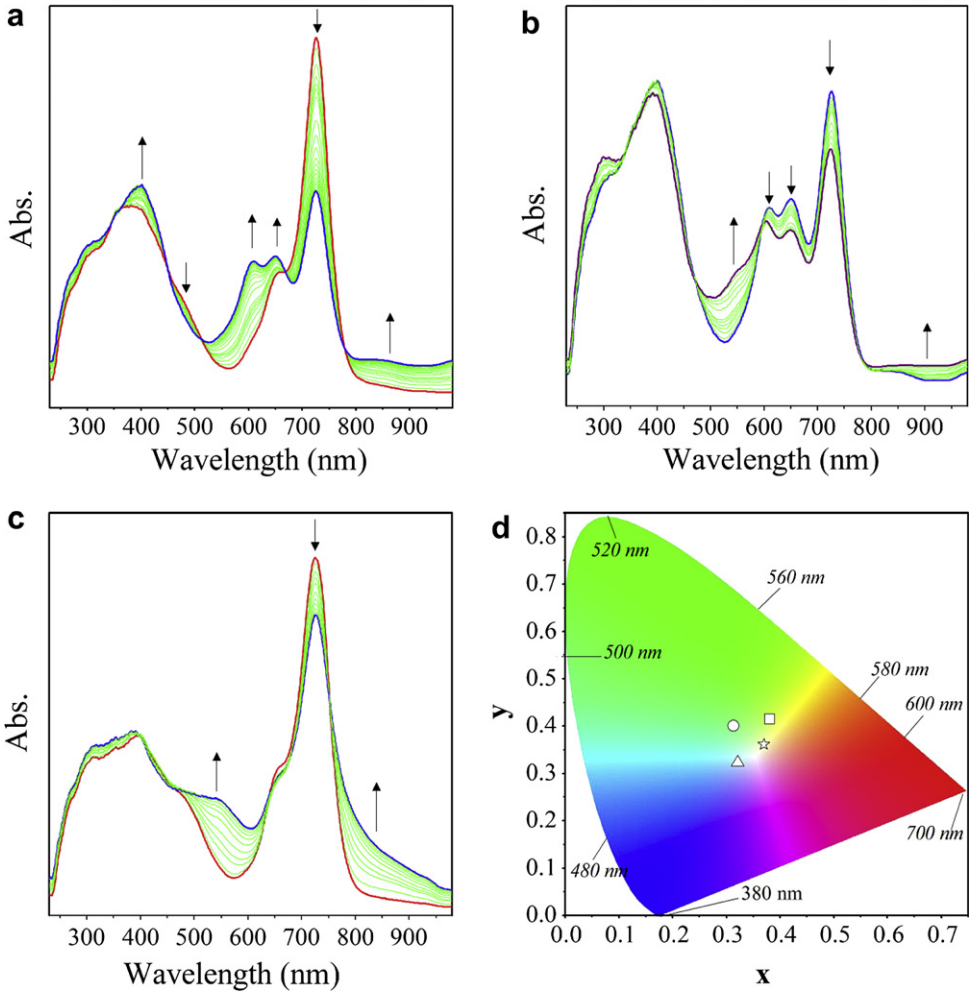

Fig. 10. *In-situ* UV–Vis spectral changes of **5**. **a**) $E_{app} = -1.40$ V. **b**) $E_{app} = -1.80$ V. **c**) $E_{app} = 0.30$ V. **d**) Chromaticity diagram (each symbol represents the color of electro-generated species; □: $Zn^{II}Pc^{-2}$, ○: $Zn^{II}Pc^{-3}$, △: $Zn^{II}Pc^{-4}$, ☆: $Zn^{II}Pc^{-1}$.

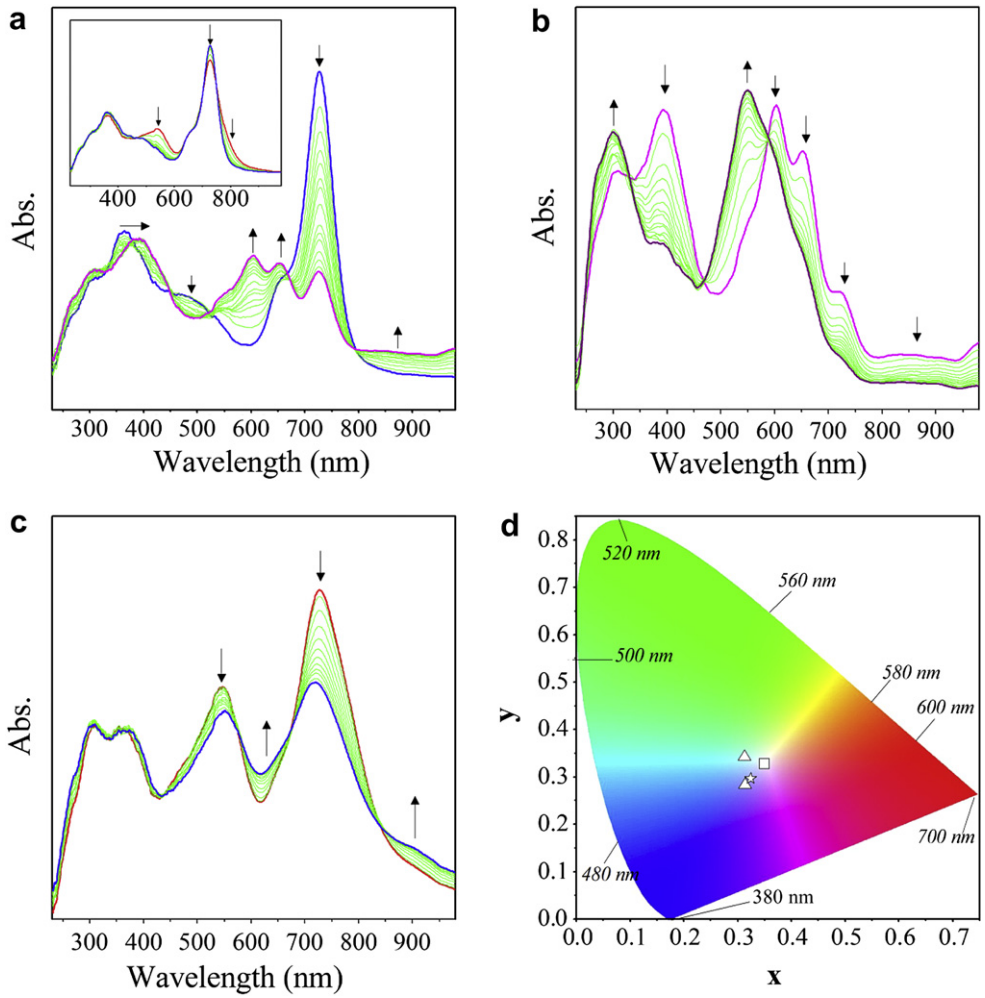

Fig. 11. *In-situ* UV–Vis spectral changes of **6**. **a**) $E_{app} = -1.40$ V (inset: $E_{app} = -0.80$ V). **b**) $E_{app} = -2.00$ V. **c**) $E_{app} = 0.60$ V. **d**) Chromaticity diagram (each symbol represents the color of electro-generated species; □: $Zn^{II}Pc^{-2}$, ○: $Zn^{II}Pc^{-3}$, △: $Zn^{II}Pc^{-4}$, ☆: $Zn^{II}Pc^{-1}$.

bands decreased in intensity which indicates decomposition of the complex under 1.00 V applied potential. Chromaticity diagram given in Fig. 10d illustrate the color coordinates of all electro-generated forms of the complex.

Fig. 11 shows the in-situ UV–Vis spectral changes of **6** under the controlled potential application. when the applied potential is −0.80 V, while the band at 540 nm decreases in intensity, the Q band increases in intensity and its broadening decreases, which indicates disaggregation of the aggregated species under applied potential (Fig. 1a inset). In the view of these spectral changes it can be concluded that the redox processes at −0.70 V ($(I_3^-/3I^-)$ in Fig. 8) is not a Pc-based process. There is no any spectral change when the applied potential is 0.40 V, which indicates that the process at 0.30 V ($(2I^-/I_2)$ in Fig. 8) is not a Pc-based oxidation process. As shown in Fig. 11a–c, the in-situ UV–Vis spectral changes under applied potential at −1.40 (Fig. 11a), −2.00 (Fig. 11b), and 0.60 (Fig. 11c) are approximately same with the spectral changes of the complex **5**. According to these spectral changes, it is easy to assign the redox processes to the electron adding or removing to the Pc ring of the complex **6**. Redox states of the complex **6** have different colors than those of the other complexes due to the presence of the band at 540 nm as shown in the chromaticity diagrams of the complex **6** (Fig. 11d). Without any potential application, while the solution of **6** is light violet ($x = 0.350$ and $y = 0.327$), the reduced and oxidized forms are bluish green ($x = 0.313$ and $y = 0.341$), bluish purple ($x = 0.315$ and $y = 0.283$) and light purple ($x = 0.325$ and $y = 0.296$) respectively as shown in Fig. 11d.

4. Conclusion

Pcs with unsaturated cinnamaldimine units directly fused to tetrapyrrole cores are successfully accomplished. Voltammetric responses of the complexes support the proposed structure of the complexes and successive change of the substituents from nitro- to amino-, 4-(dimethylamino)cinnamaldimine, and its quaternized forms. Presence of electroactive nitro, amino and cinnamaldimine groups extended the redox richness of the phthalocyanine ring which is one of the desired properties of the metal-lophthalocyanines in electrochemical technological applications. Directly conjugation of Pc ring with unsaturated cinnamaldimine groups causes a shift of the redox processes to negative side and polymerization of the complex on the working electrode. Although the complexes have different substituent environments, spectral changes during the electron transfer reactions are similar to each other and they indicate that while substituents shift the electron transfer reaction they do not affect the spectrum of the Pc-based anionic and cationic forms of the ZnPc complexes.

Acknowledgement

GKK thanks the Research Fund of Yildiz Technical University (Project No: 28-01-02-12) for partial support of this work.

References

[1] Salan Ü, Kobayashi N, Bekaroğlu Ö. Effect of peripheral substitution on the electronic absorption and magnetic circular dichroism (MCD) spectra of metal-free azo-coupled bisphthalocyanine. Tetrahedron Letters 2009;50(49):6775–8.
[2] Hanack M, Lang M. Conducting stacked metallophthalocyanines and related-compounds. Advanced Materials 1994;6(11):819–33.
[3] Cook MJ, McKeown NB, Simmons JM, Thomson AJ, Daniel MF, Harrison KJ, et al. Spectroscopic and X-ray-diffraction study of Langmuir–Blodgett-films of some 1,4,8,11,15,18-hexaalkyl–22,25-bis(carboxypropyl)-phthalocyanines. Journal of Materials Chemistry 1991;1:121–7.
[4] Schlettwein D, Wöhrle D, Jaeger NI. Reversible reduction and reoxidation of thin-films of tetrapyrazinotetraazaporphyrines. Journal of the Electrochemical Society 1989;136:2882–6.
[5] Dogo S, Germain JP, Maleysson C, Pauly A. Interaction of NO_2 with copper phthalocyanine thin-films. 2. Application to gas sensing. Thin Solid Films 1992;219:251–6.
[6] Simon J, Sirlin C. Mesomorphic molecular materials for electronics, opto-electronics, iono-electronics – octaalkyl-phthalocyanine derivatives. Pure and Applied Chemistry 1989;61:1625–9.
[7] de la Torre G, Vazquez P, Agullo-Lopez F, Torres T. Phthalocyanines and related compounds: organic targets for nonlinear optical applications. Journal of Materials Chemistry 1998;8:1671–83.
[8] Yamaguchi S, Sasaki Y. Primary process of photocarrier generation in Y-form titanyl phthalocyanine studied by electric-field-modulated picosecond time-resolved fluorescence spectroscopy. Journal of Physical Chemistry B 1999;130 (33):6835–8.
[9] de la Torre G, Claessens CG, Torres T. Phthalocyanines: old dyes, new materials. Putting color in nanotechnology. Chemical Communications 2007;20: 2000–15.
[10] Ali H, Van Lier JE. Metal complexes as photo- and radiosensitizers. Chemical Reviews 1999;99(9):2379–450.
[11] Boyle RW, Leznoff CC, Van Lier JE. Biological-activities of phthalocyanines. 16. Tetrahydroxy- and tetraalkylhydroxy zinc phthalocyanines – effect of alkyl chain-length on in vitro and in vivo photodynamic activities. British Journal of Cancer 1993;67(6):1177–81.
[12] Lever ABP, Hempstead MR, Leznoff CC, Liu W, Melnik M, Nevin WA, et al. Recent studies in phthalocyanine chemistry. Pure and Applied Chemistry 1986;58(11):1467–76.
[13] Hohnholz D, Steinbrecher S, Hanack M. Applications of phthalocyanines in organic light emitting devices. Journal of Molecular Structure 2000;521:231–7.
[14] Cong FD, Ning B, Du XG, Ma CY, Yu HF, Chen B. Facile synthesis, characterization and property comparisons of tetraaminometallophthylocyanines with and without intramolecular hydrogen bonds. Dyes and Pigments 2005;66(2): 149–54.
[15] Clarckson GJ, McKeown NB, Treacher KE. Synthesis and characterization of some novel phthalocyanines containing both oligo(ethyleneoxy) and alkyl or alkoxy side-chains – novel unsymmetrical discotic mesogens. Journal of the Chemical Society, Perkin Transactions 1 1995;14:1817–23.
[16] Duro JA, dela Torre G, Barbera J, Serrano JL, Torres T. Synthesis and liquid-crystal behavior of metal-free and metal-containing phthalocyanines substituted with long-chain amide groups. Chemistry of Materials 1996;8 (5):1061–6.
[17] Kalkan A, Bayır ZA. Synthesis and characterisation of unsymmetrical porphyrazines containing bis(hydroxyethylthio) substituents. Monatshefte für Chemie 2003;134(12):1555–60.
[18] Uslu RZ, Gul A. Porphyrazines with tosylamine functional groups. Comptes Rendus De L Academie Des Sciences Serie Ii Fascicule C-Chimie 2000;3 (8):643–8.
[19] Hamuryudan E, Bayır ZA, Bekaroglu Ö. Dioxadiaza macrocycle-substituted phthalocyanines. Dyes and Pigments 1999;43(2):77–81.
[20] Calvete M, Hanack MA. Binuclear phthalocyanine containing two different metals. European Journal of Organic Chemistry 2003;11:2080–3.
[21] Bayır ZA. Synthesis and characterization of novel soluble octa-cationic phthalocyanines. Dyes and Pigments 2005;65:235–42.
[22] Öztürk R, Güner S, Aktas B, Gül A. Synthesis, characterization and EPR studies of supramolecular porphyrazines. Supramolecular Chemistry 2005;17(3): 233–41.
[23] Dinçer HA, Gül A, Koçak MB. A novel route to 4-chloro-5-alkyl-phthalonitrile and phthalocyanines derived from it. Journal of Porphyrins and Phthalocyanines 2004;8(10):1204–8.
[24] Choi CF, Tsang PT, Huang JD, Chan EYM, Ko WH, Fong WP, et al. Synthesis and in vitro photodynamic activity of new hexadeca-carboxy phthalocyanines. Chemical Communications 2004;19:2236–7.
[25] Liu W, Jensen TJ, Fronczek FR, Hammer RP, Smith KM, Vicente MGH. Synthesis and cellular studies of nonaggregated water-soluble phthalocyanines. Journal of Medicinal Chemistry 2005;48(4):1033–41.
[26] Gursoy S, Cihan A, Koçak MB, Bekaroglu Ö. Synthesis and complexation of a novel soluble vic-dioxime ligand. Monatshefte Fur Chemie 2001;132: 967–72.
[27] Shankar R, Sharma P, Cabrera A, Espinosa G, Rosas N. Synthesis and crystal structures of some aryloxy-substituted phthalonitriles. Indian Journal of Chemistry Section B – Organic Chemistry Including Medicinal Chemistry 1996;35B(9):894–9.
[28] Wohrle D, Krawczyk G, Paliuras M. Polymeric bound porphyrins and their precursors. 6. Syntheses of water-soluble, negatively or uncharged polymers with covalently bound moieties of porphyrin derivatives. Macromolecular Chemistry and Physics 1988;189(5):1001–11.
[29] Karaoğlan GK, Gümrükcü G, Koca A, Gül A. The synthesis, characterization, electrochemical and spectroelectrochemical properties of a novel, cationic, water-soluble Zn phthalocyanine with extended conjugation. Dyes and Pigments 2011;88(3):247–56.
[30] Young JG, Onyebuagu W. Synthesis and characterization of di-disubstituted phthalocyanines. Journal of Organic Chemistry 1990;55(7):2155–9.
[31] Lunardi CN, Rotta JCG, Tedesco AC. Synthesis, photophysical and photobiological study of synergic photosensitizer: zinc-phthalocyanine with Ca^{2+} chelating agent. Current Organic Chemistry 2007;11(7):647–54.
[32] Pekbelgin Karaoglu HR, Gül A, Burkut Kocak M. Synthesis and characterization of a new tetracationic phthalocyanine. Dyes and Pigments 2008;76:231–5.
[33] Arslan S, Yilmaz I. Synthesis, electrochemistry, and in situ spectroelectrochemistry of a new water-soluble zinc phthalocyanine substituted with naphthoxy-4-sulfonic acid sodium salt. Transition Metal Chemistry 2007;32 (3):292–8.
[34] Kobayashi N, Ashida T, Osa T. Synthesis, spectroscopy, electrochemistry, and spectroelectrochemistry of a zinc phthalocyanine with D(2h) symmetry. Chemistry Letters 1992;10:2031–4.
[35] Acar I, Bıyıklıoğlu Z, Koca A, Kantekin H. Synthesis, electrochemical, in situ spectroelectrochemical and in situ electrocolorimetric characterization of new metal-free and metallophthalocyanines substituted with 4-{2-[2-(1-naphthyloxy)ethoxy]ethoxy} groups. Polyhedron 2010;29:1475–84.
[36] Sivanesan A, John SA. Amino group positions dependent morphology and coverage of electropolymerized metallophthalocyanine (M = Ni and Co) films on electrode surfaces. Electrochimica Acta 2008;53:6629–63.
[37] Rodrigues C, Batista AA, Aucelio RQ, Teixeira LR, Visentin LD, Beraldo H. Spectral and electrochemical studies of ruthenium(II) complexes with N4-methyl-4-nitrobenzaldehyde and N4-methyl-4-nitrobenzophenone thiosemicarbazone: potential anti-trypanosomal agents. Polyhedron 2008;27:3061–6.
[38] Pospisil L, Hromadova M, Sokolová R, Bulickova J, Fanelli N. Cationic catalysis and hidden negative differential resistance in reduction of radical anion of nitrobenzene. Electrochimica Acta 2008;53:4852–8.
[39] Carlier R, Raoult E, Tallec A, Andre V, Gauduchon P, Lancelot JC. Electrochemical behavior of mutagenic nitro and amino derivatives of carbazole. Electroanalysis 1997;9(1):79–84.
[40] Kandaz M, Michel SLJ, Hoffman BM. Functional solitare- and trans-hybrids, the synthesis, characterization, electrochemistry and reactivity of porphyrazine/phthalocyanine hybrids bearing nitro and amino functionality. Journal of Porphyrins and Phthalocyanines 2003;7(9–10):700–12.
[41] Gruber J, Camilo FF. Synthesis of novel diaryloxocyclopentanethiocarboxylates by electrochemical reduction of cinnamic acid thioesters. Journal of the Chemical Society, Perkin Transactions 1 1999;2:127–9.
[42] Matesanz AI, Mosa J, Garcia I, Pastor C, Souza P. Synthesis, characterization, crystal structure and electrochemistry of a novel palladium(II) binuclear complex containing 1,2,4-triazole bis(4-phenylthiosemicarbazone) bridges. Inorganic Chemistry Communications 2004;7(6):756–9.
[43] Arquero A, Mendiola MA, Souza P, Sevilla MT. Synthesis, spectral and electrochemical properties of divalent metal complexes containing thiohydrazone and thiosemicarbazone ligands. Polyhedron 1996;15(10):1657–65.
[44] Yaraliyev YA. Oxidation of iodide ions by means of cyclic voltammetry. Electrochimica Acta 1984;29(9):1213–4.
[45] Lopez B, Iwasita T, Giordano MC. Electrochemical behavior of iodide–iodine and bromide–bromine redox systems in nitromethane solutions. Journal of Electroanalytical Chemistry 1973;47(3):469–78.
[46] Dinçer HA, Koca A, Gül A, Burkut Koçak M. Novel phthalocyanines bearing both quaternizable and bulky substituents. Dyes and Pigments 2008;76 (3):825–31.
[47] Obirai J, Nyokong T. Synthesis, spectral and electrochemical characterization of mercaptopyrimidine-substituted cobalt, manganese and Zn(II) phthalocyanine complexes. Electrochimica Acta 2005;50:3296–304.
[48] Koca A, Özkaya AR, Selcukoglu M, Hamuryudan E. Electrochemical and spectroelectrochemical characterization of the phthalocyanines with pentafluorobenzyloxy substituents. Electrochimica Acta 2007;52(7):2683–90.
[49] Koca A, Bayar S, Dinçer HA, Gonca E. Voltammetric, in-situ spectroelectrochemical and in-situ electrocolorimetric characterization of phthalocyanines. Electrochimica Acta 2009;54(10):2684–92.
[50] Lever ABP, Milaeva ER, Speier G. Phthalocyanines: properties and applications. In: Leznoff CC, Lever ABP, editors. The redox chemistry of metallophthalocyanines in solution, vol. 3. New York: VCH; 1993.
[51] Simicglavaski B, Zecevic S, Yeager E. Spectroelectrochemical in situ studies of phthalocyanines. Journal of the Electrochemical Society 1987;134(3): C130.